

# Upwash exploitation and downwash avoidance by flap phasing in ibis formation flight

Steven J. Portugal<sup>1</sup>, Tatjana Y. Hubel<sup>1</sup>, Johannes Fritz<sup>2</sup>, Stefanie Heese<sup>2</sup>, Daniela Trobe<sup>2</sup>, Bernhard Voelkl<sup>2,3,†</sup>, Stephen Hailes<sup>1,4</sup>, Alan M. Wilson<sup>1</sup> & James R. Usherwood<sup>1</sup>

Many species travel in highly organized groups<sup>1–3</sup>. The most quoted function of these configurations is to reduce energy expenditure and enhance locomotor performance of individuals in the assemblage<sup>4–11</sup>. The distinctive V formation of bird flocks has long intrigued researchers and continues to attract both scientific and popular attention<sup>4,7,9–14</sup>. The well-held belief is that such aggregations give an energetic benefit for those birds that are flying behind and to one side of another bird through using the regions of upwash generated by the wings of the preceding bird<sup>4,7,9–11</sup>, although a definitive account of the aerodynamic implications of these formations has remained elusive. Here we show that individuals of northern bald ibises (*Geronticus eremita*) flying in a V flock position themselves in aerodynamically optimum positions, in that they agree with theoretical aerodynamic predictions. Furthermore, we demonstrate that birds show wingtip path coherence when flying in V positions, flapping spatially in phase

and thus enabling upwash capture to be maximized throughout the entire flap cycle. In contrast, when birds fly immediately behind another bird—in a streamwise position—there is no wingtip path coherence; the wing-beats are in spatial anti-phase. This could potentially reduce the adverse effects of downwash for the following bird. These aerodynamic accomplishments were previously not thought possible for birds because of the complex flight dynamics and sensory feedback that would be required to perform such a feat<sup>12,14</sup>. We conclude that the intricate mechanisms involved in V formation flight indicate awareness of the spatial wake structures of nearby flock-mates, and remarkable ability either to sense or predict it. We suggest that birds in V formation have phasing strategies to cope with the dynamic wakes produced by flapping wings.

Theories of fixed-wing aerodynamics have predicted the exact spanwise positioning that birds should adopt in a V formation flock to

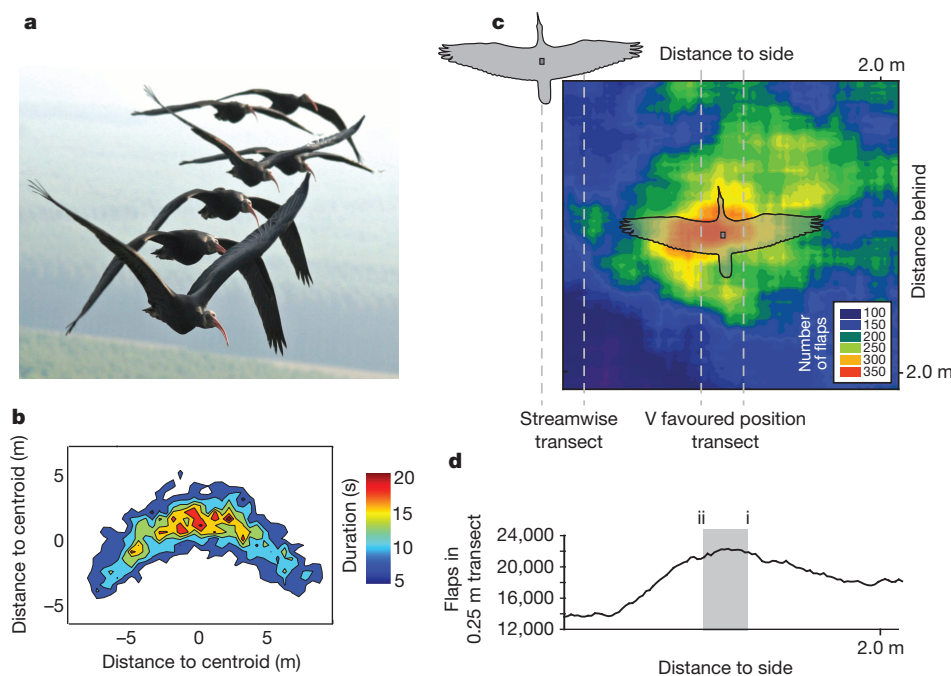


**Figure 1 | V formation flight in migrating ibises.** **a**, Northern bald ibises (*G. eremita*) flying in V formation during a human-led migratory flight (photograph M. Unsöld). **b**, Three-dimensional location histogram of the 7 min flight section, showing position of individual ibises ( $n = 14$ ) in the V formation, with respect to flock centroid, measured by a 5 Hz GPS data logger. The colour scale refers to the duration (in seconds) a bird was present in each  $0.25 \text{ m} \times 0.25 \text{ m}$  grid. A plot detailing the formation shape for the duration of the entire flight can be found in Supplementary Fig. 7. **c**, Histogram of number

of flaps (colour coded) recorded in each  $0.25 \text{ m} \times 0.25 \text{ m}$  region between all birds and all other birds. Most flaps occurred at an angle of approximately  $45^\circ$  to the bird ahead (or behind). Transects denoted by dashed lines, directly behind or along the most populated V favoured position (just inboard of wingtip to wingtip), are the same as those detailed in Fig. 3. **d**, Histogram detailing the total number of flaps recorded between each bird–bird pair, with respect to position of the following bird. The shaded area (ii–i) denotes the limits of optimal relative positioning, based on fixed-wing aerodynamics.

<sup>1</sup>Structure & Motion Laboratory, the Royal Veterinary College, University of London, Hatfield, Hertfordshire AL9 7TA, UK. <sup>2</sup>Waldrappteam, Schulgasse 28, 6162 Mutters, Austria. <sup>3</sup>Institute for Theoretical Biology, Humboldt University at Berlin, Invalidenstrasse 43, 10115 Berlin, Germany. <sup>4</sup>Department of Computer Science, University College London, Gower Street, London WC1E 6BT, UK. †Present address: Edward Grey Institute, Department of Zoology, University of Oxford, Oxford OX1 3PS, UK.

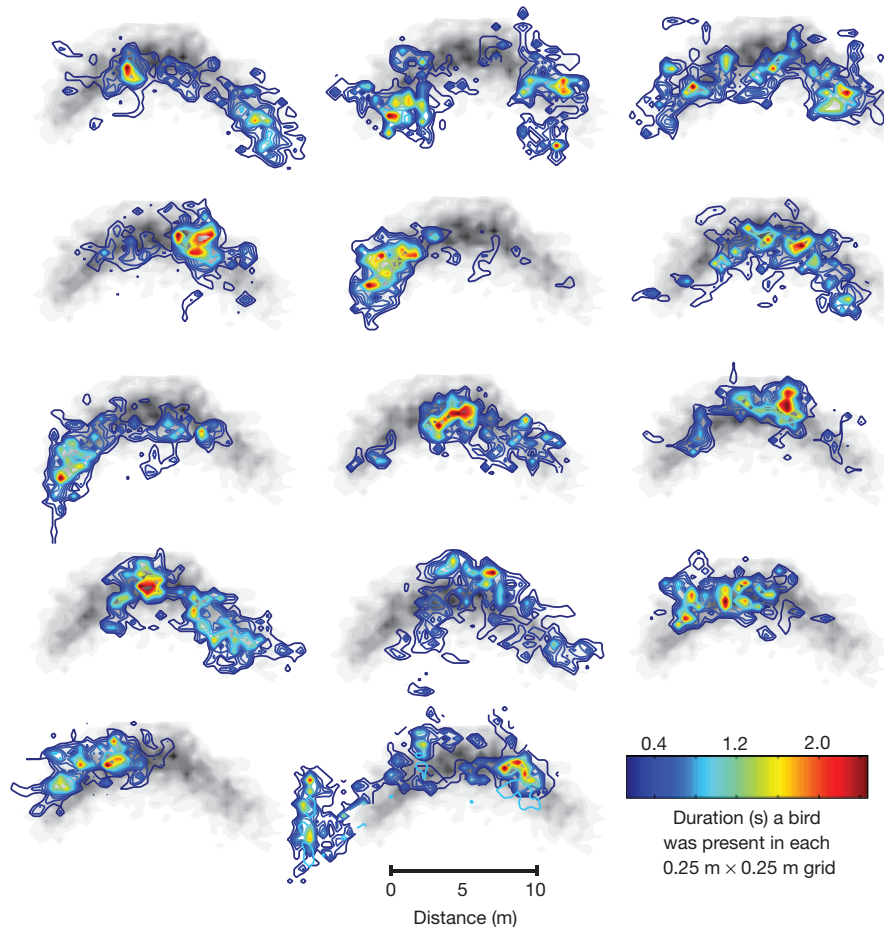


**Figure 2 | Histograms demonstrating the positional infidelity for each northern bald ibis in the V formation during the migratory flight.** The grey shaded V shape behind each individual histogram ( $n = 14$ ) denotes the structure for all individuals in the flock (see Fig. 1b). The colour code refers to

maximize upwash capture<sup>4,9–14</sup>. The primary empirical evidence confirming that this mechanism is used is a reduction in heart rate and wing-beat frequency in pelicans flying in a V formation<sup>7</sup>. There is a general lack of experimental data from free-flying birds, mainly because of the complications of measuring the intricate and three-dimensional complexity of formation flight, and the lack of appropriate devices to monitor and record such information. Therefore, the precise aerodynamic interactions that birds use to exploit upwash capture have not been identified. To investigate the purported aerodynamic interactions of V formation flight, we studied a free-flying flock of northern bald ibises (*Geronticus eremita*) (Fig. 1a), a critically endangered migratory species. We used new technology<sup>15,16</sup> to measure the position, speed and heading of all birds in a V formation. We recorded position and every wing flap of 14 birds during 43 min of migratory flight using back-mounted integrated global positioning system (GPS) (5 Hz) and inertial measurement units (300 Hz) (see Methods)<sup>15,16</sup>. The precision of these measurements allows the relative positioning of individuals in a V to be tracked, and the potential aerodynamic interactions to be investigated at a level and complexity not previously feasible.

During a 7 min section of the flight, where most of the flock flew in approximate V formation in steady, level and planar direct flight (see Methods), we found wing flaps occurred at an angle of, on average,  $45^\circ$  to the bird ahead (or behind), and approximately 1.2 m behind (Fig. 1b–d). The most populated  $1\text{ m} \times 1\text{ m}$  region was 0.49–1.49 m behind and to the side of the bird ahead. The centre of the most populated (0.25 m) spanwise region was at 0.904 m, resulting in a wingtip overlap<sup>9–13</sup> of 0.115 m (Fig. 1c,

the duration (in seconds) a bird was present in each  $0.25\text{ m} \times 0.25\text{ m}$  grid. Although individual birds showed some bias towards the front, back, left or right regions of the V formation, these positions were not maintained rigidly.

d; wingspan  $b = 1.2\text{ m}$ ). This falls within the bounds of predictions of fixed-wing theory<sup>9–13</sup> for maximizing the benefits from upwash, which range from zero wingtip overlap (assuming no wake contraction<sup>4</sup>) to, maximally, 0.13 m (assuming elliptical loading over the pair of wings, and full wake contraction from wingspan  $b$  to  $\pi b/4$ )<sup>9</sup>.

During this 7 min section of V formation flight, individual birds show a certain degree of positional infidelity in the V flock (Fig. 2; see also Supplementary Fig. 1 and Supplementary Video 1). Although individuals contribute to the statistical V formation, their positioning is inconsistent. Certain individuals showed general preferences for a particular area in the V formation, but the variability in positioning in the flock resulted in no clear leader (see Supplementary Information for further discussion).

Although we observe that, when flying in a V, ibises position themselves in locations predicted mathematically from fixed-wing aerodynamics<sup>4,9–11</sup>, the wake of flapping birds (in this study, ibises spent 97% of their time flapping; see Methods) is likely to be complex<sup>9–14</sup>. Wingtip path coherence, where a flying object flaps its wings in spatial phase with that of the individual it is following, has been proposed as a method that would maximize upwash capture in V formation flight of birds and flying robotic devices<sup>12</sup>. Whether birds are able to take advantage of this extra level of complexity present in flapping flight (compared with that of fixed-wing flight) has remained unanswered so far.

In the ibis flock, individual flaps for each bird were described from the dorsal acceleration signal from the inertial measurement unit<sup>15</sup>. The temporal phase  $\phi_{\text{temporal}}$  is defined here as the proportion of a flap cycle of a leading bird at which a following bird initiates a flap. Spatial

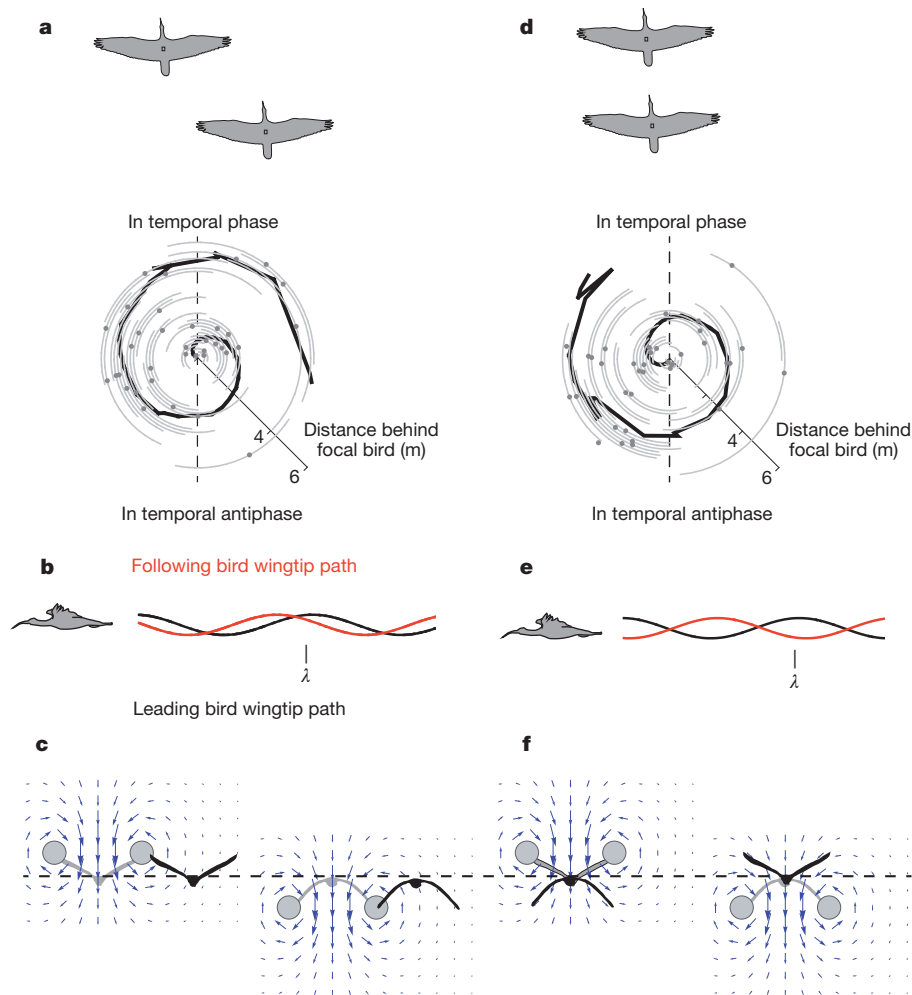


**Figure 3 | Geometric and aerodynamic implications of observed spatial phase relationships for ibises flying in a V formation.** Temporal phase increases as a function of position behind more advanced birds (median  $\pm$  95% confidence intervals of phase for each mean bird–bird interaction in a region). When positioned close to a wavelength in line with the V favoured position (a–c), wingtip paths approximately match: observed temporal phases agree with those predicted from the significant spatial phase relationship (thick black lines,  $\pm$  95% confidence intervals) at the most populated 1 m  $\times$  1 m region, using the mean wavelength measured for each position. When positioned directly in line (d–f), following birds flap in spatial antiphase, maximally separating wingtip paths. In this case the model line is derived from the median spatial phase for all bird–bird interactions up to 4 m directly behind. Induced flow velocities (blue

arrows, c, f), caused by the trailing wingtip vortices of the bird ahead (vortex cores denoted by grey circles), are modelled as infinitely long, parallel vortex filaments. Birds flying in typical V formation keep their wings close to the region of maximal induced upwash (c) throughout the flap cycle. Birds flying directly behind flap in spatial antiphase, potentially reducing the adverse effects of downwash (f), both in terms of magnitude and direction. For scale, the downwash directly between the vortices would be  $(-0.3 \text{ m s}^{-1})$ , between trailing vortices behind a bird of mass 1.3 kg, span 1.2 m at a speed of  $15 \text{ m s}^{-1}$  (no account is taken of flapping, viscosity or wake contraction). Alternative representations of a and d as Cartesian plots can be found in Supplementary Fig. 3, and Supplementary Fig. 4 details the extended data array shown beyond the presented model line.

phase  $\phi_{\text{spatial}}$  makes use of the temporal phases, and takes account of the number of wavelengths,  $\lambda$ , between the bird ahead and the bird behind:

$$\phi_{\text{spatial}} = \phi_{\text{temporal}} - 2\pi\lambda.$$

A spatial phase of zero would indicate that, were the birds to be directly following each other, the wingtip paths would match.

In the most populated 1 m  $\times$  1 m favoured V position (Fig. 1c), Rayleigh's test<sup>17</sup> for circular statistics indicates a significant unimodal bias in both temporal (Rayleigh,  $P = 0.018$ , mean phase = 0.857; Hodges–Ajne's test,  $P = 0.012$ ) and, more strongly, spatial (Rayleigh,  $P = 0.003$ , mean phase =  $-1.155$ ; Hodges–Ajne,  $P = 0.004$ ) phases (Fig. 3a, b) (see Supplementary Table 1 for further statistics; Supplementary Figs 2a, 3a and 4a). Flapping in spatial phase indicates that the wing of a following bird goes up and down tracking the path through the air previously described by the bird ahead. The following bird then benefits from consistently flapping into

the upwash region from the preceding bird (Fig. 3b, c), presumably reducing the power requirements for weight support<sup>12,14</sup>.

In contrast, birds flying directly behind, tracking the bird ahead in a streamwise position (sampled region 0.5 m across, 4 m streamwise, Fig. 1c), flap in close to spatial antiphase (median = 2.897, where precise antiphase would be  $\pm 3.142$ ), significantly ( $P < 0.05$ ) deviating from flapping 'in' spatial phase (see Supplementary Table 1 for further statistics; Supplementary Figs 2b, 3b and 4b). As such, the wingtip paths of the following bird do not match those of the preceding bird, and the wingtip paths are close to maximally separated. Birds flying directly behind another one in a streamwise location flap in spatial antiphase (Fig. 3d, e; see also Supplementary Figs 2b and 3b), potentially reducing the adverse effects of downwash (Fig. 3f), both in terms of magnitude and direction. If this position was aerodynamically adaptive, it would be predicted to be favoured at higher speeds, where parasite power is relatively high<sup>18</sup>, compared with the induced power costs of weight support; forms of slipstreaming can reduce the drag experienced by followers<sup>5,6,8,19</sup>, even in cases where there is zero net

horizontal momentum flux in the wake (that is, drag = thrust)—as in steady swimming—owing to temporal or local spatial<sup>15,20,21</sup> fluctuations from mean wake conditions. Whether the position immediately behind is accidental or intentional, and whether it offers any aerodynamic advantage or cost, is currently unclear. However, the wing-beat phasing observed when in this position would serve to displace the following bird's wings from regions of greatest downwash (presumably immediately inboard of the trailing wingtip vortices, close to wingtip paths described by the previous bird), through most of the flap cycle.

In transects both directly streamwise and along the favoured V position (Fig. 1c), temporal phase increases proportionally with distance behind the focal bird (Fig. 3a, d), with a full  $2\pi$  cycle change in phase over a complete wavelength; spatial phase is approximately maintained up to 4 m behind the leading bird. Previously, there was much uncertainty about spatial wing-beat phasing and wingtip path coherence in flapping organisms. The only previous biological evidence of this phenomenon has come from tethered locusts, where distance manipulations between a leading locust and a follower altered the phase patterns of their wing-beats<sup>22,23</sup>. Physical models also support the potential for aerodynamic advantage due to phasing: appropriate timing between tandem flapping in model dragonfly wings improves aerodynamic efficiency<sup>24</sup>. Theoretical engineering models have taken into consideration flapping flight, and the extra benefits a flapping wing may accrue in formation flight<sup>12,14</sup>. Such models have suggested that upwards of 20% variation exists in the induced power savings to be gained, if flapping is done optimally in spatial phase, compared with out of phase<sup>12</sup> (Supplementary Fig. 4).

Here we have shown that ibis flight in V formation does, on average, match predictions of fixed-wing aerodynamics (Fig. 1c, d), but that flock structure is highly dynamic (Fig. 2). Further, temporal phasing of flapping relates both to streamwise and to spanwise position. This indicates remarkable awareness of, and ability to respond to, the wing-path—and thereby the spatial wake structure—of nearby flock-mates. Birds flying in V formation flap with wingtip path coherence—the wingtips take the same path—placing wings close to the oscillating positions of maximal upwash. In contrast, birds flying in line flap in spatial antiphase—the wingtip paths are maximally separated—consistent with avoidance of adverse downwash. This raises the possibility that, in contrast to conventional aircraft, following birds may be able to benefit from 'drafting' while, to a certain extent, avoiding an increased cost of weight support by evading localized regions of downwash. Optimal flight speeds would differ between solo flight, V formation flight and (whether net-beneficial or not) in-line flight, potentially providing some account for the unstable, dynamic nature of V formation flocks.

## METHODS SUMMARY

**Measurements.** We equipped 14 juvenile northern bald ibises with back-mounted synchronized GPS (5 Hz) and inertial measurement units (300 Hz), mass 23 g (Supplementary Fig. 8), which were custom made in our laboratory, and tested and validated for accuracy and precision<sup>15,16</sup>. At the start of migration, the mass of the birds was  $1.30 \pm 0.73$  kg, the 23 g loggers constituting approximately 3% of the body mass of the smallest bird. This is below the recommended 5% for flying animals<sup>25</sup>. The ibises formed part of a large-scale conservation programme. They had been hand-reared at Zoo Vienna (Austria), imprinted onto human foster parents and taught to follow a powered parachute (paraplane) to learn the migration routes (Methods). Experimental protocols were approved by the Royal Veterinary College local Ethics and Welfare Committee. A GPS trace of the ibis flight imposed over Google Earth (Landsat) can be found in Supplementary Data 1 as a KML file. GPS data were post-processed using GravNav Waypoint™ software<sup>15,26</sup>, and inertial measurement unit data by custom-written MATLAB (R2012b, Mathworks) programs<sup>16,26</sup>. Mean flap frequency, speed and peak detection protocols are detailed in Supplementary Figs 5 and 6. For further details on post-processing, see Methods.

**Statistical analysis.** Circular statistics<sup>17</sup> were done in LabVIEW (National Instruments). First-order (Rayleigh test) and second-order (Hodges–Ajne) statistics were

used to test the phasing of wing beats for significant deviations from random distribution. For further details on statistical analysis, see Methods.

**Online Content** Any additional Methods, Extended Data display items and Source Data are available in the online version of the paper; references unique to these sections appear only in the online paper.

**Received 30 May; accepted 3 December 2013.**

- Couzin, I. D., Krause, J., Franks, N. R. & Levin, S. A. Effective leadership and decision-making in animal groups on the move. *Nature* **433**, 513–516 (2004).
- Nagy, M., Akos, Z., Biro, D. & Vicsek, T. Hierarchical group dynamics in pigeon flocks. *Nature* **464**, 890–894 (2010).
- May, R. M. Flight formations in geese and other birds. *Nature* **282**, 778–780 (1979).
- Lissaman, P. B. & Schollenberger, C. A. Formation flight of birds. *Science* **168**, 1003–1005 (1970).
- Liao, J. C., Beal, D. N., Lauder, G. V. & Triantafyllou, M. S. Fish exploiting vortices decrease muscle activity. *Science* **302**, 1566–1569 (2003).
- Bill, R. G. & Hernnkind, W. F. Drag reduction by formation movement in spiny lobsters. *Science* **193**, 1146–1148 (1976).
- Weimerskirch, H., Martin, J., Clerquin, Y., Alexandre, P. & Jiraskova, S. Energy saving in flight formation. *Nature* **413**, 697–698 (2001).
- Fish, F. E. Kinematics of ducklings swimming in formation: consequence of position. *J. Exp. Zool.* **273**, 1–11 (1995).
- Badgerow, J. P. & Hainsworth, F. R. Energy savings through formation flight? A re-examination of the vee formation. *J. Theor. Biol.* **93**, 41–52 (1981).
- Cutts, C. J. & Speakman, J. R. Energy savings in formation flight of pink-footed geese. *J. Exp. Biol.* **189**, 251–261 (1994).
- Hummel, D. Aerodynamic aspects of formation flight in birds. *J. Theor. Biol.* **104**, 321–347 (1983).
- Willis, D. J., Peraire, J. & Breuer, K. S. in *Proc. 25th American Institute of Aeronautics and Astronautics Appl. Aerodynam. Conf.* <http://doi.org/10.2514/6.2007-4182> (2007).
- Hainsworth, F. R. Precision and dynamics of positioning by Canada geese flying in formation. *J. Exp. Biol.* **128**, 445–462 (1987).
- Maeng, J. S. *et al.* A modelling approach to energy savings of flying Canada geese using computational fluid dynamics. *J. Theor. Biol.* **320**, 76–85 (2013).
- Usherwood, J. R., Stavrou, M., Lowe, J. C., Roskilly, K. & Wilson, A. M. Flying in a flock comes at a cost in pigeons. *Nature* **474**, 494–497 (2011).
- Wilson, A. M. *et al.* Locomotion dynamics of hunting in wild cheetahs. *Nature* **498**, 185–189 (2013).
- Fisher, N. I. *Statistical Analysis of Circular Data* Ch. 4, 59–102 (Cambridge Univ. Press, 1993).
- Pennycuik, C. J. *Bird Flight Performance: A Practical Calculation Manual* Ch. 3, 37–78 (Oxford Univ. Press, 1989).
- Spence, A. J., Thurman, A. S., Maher, M. J. & Wilson, A. M. Speed, pacing and aerodynamic drafting in thoroughbred horse racing. *Biol. Lett.* **8**, 678–681 (2012).
- Chatard, J.-C. & Wilson, B. Drafting distance in swimming. *Med. Sci. Sports Exerc.* **35**, 1176–1181 (2003).
- Delextrat, A. *et al.* Drafting during swimming improves efficiency during subsequent cycling. *Med. Sci. Sports Exerc.* **35**, 1612–1619 (2003).
- Kutsch, W., Camhi, J. & Sumbre, G. Close encounters among flying locusts produce wing-beat coupling. *J. Comp. Physiol. A* **174**, 643–649 (1994).
- Camhi, J. M., Sumbre, G. & Wendler, G. Wing-beat coupling between flying locusts pairs: preferred phase and life enhancement. *J. Exp. Biol.* **198**, 1051–1063 (1995).
- Usherwood, J. R. & Lehmann, F. Phasing of dragonfly wings can improve efficiency by removing swirl. *J. R. Soc. Interface* **5**, 1303–1307 (2008).
- White, C. R. *et al.* Implantation reduces the negative effects of bio-logging on birds. *J. Exp. Biol.* **216**, 537–542 (2013).
- King, A. J. *et al.* Selfish-herd behaviour of sheep under threat. *Curr. Biol.* **22**, R561–R562 (2012).

**Supplementary Information** is available in the online version of the paper.

**Acknowledgements** The Waldrapteam assisted with data collection and provided logistical support (J.F., B.V.). We thank members of the Structure & Motion Laboratory for discussions and assistance, particularly J. Lowe, K. Roskilly, A. Spence and S. Amos, and C. White and R. Bompfrey for reading an earlier draft of the paper. Funding was provided by an Engineering and Physical Sciences Research Council grant to A.M.W., J.R.U. and S.Ha. (EP/H013016/1), a Biotechnology and Biological Sciences Research Council grant to A.M.W. (BB/J018007/1) and a Wellcome Trust Fellowship (095061/Z/10/Z) to J.R.U.

**Author Contributions** S.J.P., S.Ha., A.M.W. and J.R.U. developed the concept of the paper. J.F., S.He. and D.T. reared and trained the birds. S.J.P., S.He., D.T., B.V. and J.F. collected the field data. S.J.P., T.Y.H. and J.R.U. undertook the data processing and analyses; J.R.U. performed the circular statistics. S.J.P., T.Y.H., A.M.W. and J.R.U. wrote the manuscript, with input from all authors.

**Author Information** Reprints and permissions information is available at [www.nature.com/reprints](http://www.nature.com/reprints). The authors declare no competing financial interests. Readers are welcome to comment on the online version of the paper. Correspondence and requests for materials should be addressed to S.J.P. (SPortugal@rvc.ac.uk).

## METHODS

**Birds.** Northern bald ibises (*G. eremita*) ( $n = 14$ , five females and nine males) were hatched at Zoo Vienna, Austria, in March 2011, and imprinted immediately onto human foster parents (S.He. and D.T.). At 4 months of age, the birds began training flights behind a powered parachute (paraplane). Training flights lasted between 1 and 4 h, and were up to 5 km in length. At the end of July, birds were fitted with dummy loggers to prepare them for being equipped with data loggers for the long-distance migratory flights. The mass of the birds at the start of migration was  $1.30 \pm 0.73$  kg. As such, the 23 g loggers constituted approximately 3% of the body mass of the smallest bird. This is comfortably below the recommended 5% for flying animals<sup>25,27</sup>. Experimental protocols were approved by the Royal Veterinary College local Ethics and Welfare Committee. The loggers were externally attached, using Velcro and a harness (Supplementary Fig. 8). The dummy loggers remained on when birds were at rest in the aviary, which was at all times apart from the migratory flights. The first migratory flight began in August. The total migratory flight plan was from the training site near Salzburg, Austria ( $47.75377^\circ$  N,  $13.052959^\circ$  E), to Orbetello, Italy ( $42.425484^\circ$  N,  $11.232662^\circ$  E). Once en route, birds were flown, on average, every third day. During flights, the birds followed the paraplane, but were typically to the side of the vehicle, on average 147 m laterally, consistently to the left, except for one turn (see Supplementary Figs 5 and 6). All loggers functioned fully. The birds were flown early in the morning (7:00 departure); later flight times increased the occurrence of thermalling and gliding, resulting in the birds not following the paraplane sufficiently. A GPS trace of the full flight, imposed over Google Earth (Landsat), can be seen in Supplementary Data 1 (as a KML file). The recorded flight was the second stage of the migration.

**Data loggers.** Further information about the loggers can be found in refs 15 and 16. Briefly, GPS was recorded at 5 Hz and data were post-processed differentially over the short baseline between base station and ibises, using Waypoint GrafNav 8.10. L1 coarse/acquisition (C/A) code pseudo-range measurements were used to calculate the position of each GPS logger, with velocity determined from L1 Doppler measurements. Using this approach can provide positional accuracy to 0.3 m and speed accuracy better than  $0.1 \text{ m s}^{-1}$ . Accelerometer data were recorded at 300 Hz.

**Initial data processing.** The flight was checked for any periods when the birds had maintained periods of circling flight (note we do include one circle in our sequence) through examination of the GPS and accelerometer traces, and these sections were removed (less than 4 min of the total flight duration). The remaining flight, therefore, consisted of straight-line flight. The take-off and landing periods were removed, as, when taking off, it took approximately 4 min for the birds to form a coherent flock, and to follow the paraplane. Similarly, when the paraplane began to descend at the end of the flight, the birds separated and began to glide during descent. The position of the paraplane was recorded and tracked by a data logger (see Supplementary Figs 5 and 6). The GPS, recorded at 5 Hz, was interpolated (MATLAB, R2012b, Mathworks) to the same sampling rate as the accelerometer data, at 300 Hz. The interpolation replaced missing values in the GPS. GPS and accelerometer data were passed through a fourth-order Butterworth filter (MATLAB). To produce the histograms (Fig. 1b, c), the original GPS values were used after being interpolated to a constant 5 Hz sampling frequency. In Figs 1b and 2, the colour scale refers to the duration a bird was present in each  $0.25 \text{ m} \times 0.25 \text{ m}$  grid. For Fig. 1c, the colour scale refers to the number of flaps recorded in each grid. In Fig. 1c, the regional transect labelled 'streamwise transect' is offset because, for display and analysis, all data from the left side are mirrored to the right so all data points are on one side; thus the centre of the first sampled region lies  $0.125 \text{ m}$  behind and to the right of the lead bird. Dorsal acceleration was used to determine each wing flap, and the upper reversal point<sup>28</sup> of the flap cycle (see Supplementary Figs 5 and 6). Note that this reversal point in acceleration of the back need not relate to peak wing elevation—or indeed any particular wing kinematic—for the phasing analysis to function.

**Height.** Height was recorded. The precision of height measurements, however, is lower than for horizontal positions<sup>29</sup>. This is because there were no satellites below the birds, and this geometry of the satellites caused a reduction in precision<sup>29</sup>. We do not consider vertical position because of the small 'signal' of interest (very slight vertical deflections) compared with the relatively high 'noise' (inevitable because of GPS satellite geometry). We chose a section where, according to the available error measurement calculated by Waypoint (see 'Data loggers'), the height values were relatively consistent and that during this flight portion the birds were flying close to the same horizontal plane.

**Calculating flock formation and individual positioning.** To establish positioning of individuals and structure in the flock, a flock centroid was determined. To calculate the centroid of the flock, the MATLAB function 'centroid' was used. This function calculates the centroid of a polygon. The MATLAB centroid function treated each bird as a point of a polygon, and determined the centroid for each time point. An average speed was calculated and any birds with a speed discrepancy

higher than  $3 \text{ m s}^{-1}$  away from the mean flock speed were removed for that time point. From this, the resultant centroid was calculated now containing only birds close in position and speed. A rotation matrix was applied to the data to re-orient the heading so all birds were heading 'up', and the direction of the centroid was always in the positive 'Y' direction. The resultant matrix comprised a position for each bird for each sampling point. Theta ( $\theta$ ), the angle between each bird and the lead bird, was calculated, transforming Cartesian to polar coordinates (cart2pole, MATLAB). For data presentation in the histograms (Fig. 1b), the field of view was set to  $15 \text{ m} \times 15 \text{ m}$ , and the area was divided into a  $60 \times 60$  grid of bins ( $0.25 \text{ m} \times 0.25 \text{ m}$ ). Position 0/0 is the centroid. The heat histograms are shown as contour plots with five contour levels.

During the 7 min section of V formation flight, individual birds showed a certain degree of positional infidelity in the V flock (Fig. 2; see also Supplementary Fig. 1 and Supplementary Video 1). Although individuals contributed to the statistical V formation, their positioning was inconsistent. Certain individuals showed general preferences for a particular area in the V formation, whether left, right, front or rear, but the variability in positioning resulted in no clear leader in the flock (Fig. 2). Navigational ability and kin selection have been proposed as principal drivers of leadership in V formation flight<sup>30</sup>, with more experienced birds or parents of a family group taking the lead<sup>30</sup>. The ibis flock in the present study comprised birds of the same age ( $< 1$  yr old), with no previous navigational experience of the route and no parent-offspring relationships. The absence of immediate kin selection and learnt navigational ability as possible factors determining a V formation structure in the recorded flight strengthens the evidence for an aerodynamic function behind the V formation observed in the ibis. The young age of the birds, however, may be the main factor why there was a lack of a clear leader in the ibis flock, contrasting with previous observations of adult ibises, in which consistent leaders in flocks were identified<sup>31</sup>. Spontaneous and inconsistent leadership has been identified in bird flocks either where no consistent social hierarchy exists<sup>32</sup>, or when no previous knowledge of a route is known<sup>33</sup>. For other 'classic' V formation fliers, the first migration is a significant cause of mortality for young birds, even when migrating with parents. As such, aerodynamic mechanisms that reduce the energetic cost of (albeit only very infrequent) migratory flight may present considerable selection advantage.

**Movement in flock.** Movement in the V formation was investigated by taking a  $45^\circ$  line, the preferred angle for positioning with the V (Fig. 1c) as a transect from the apex of the V. The apex was determined by the intersection of two  $45^\circ$  lines, down each side of the V formation. For every bird for each time point, we measured how far it was positioned from the  $45^\circ$  perpendicular transect line. For simplicity of analysis, all data were flipped (mirrored) so they could all be plotted against one  $45^\circ$  line. In Supplementary Fig. 1a, the red circles represent the original positions of the birds, for all birds and all times. From this, the shortest distance to the  $45^\circ$  line was calculated (blue line) and the position was projected on the  $45^\circ$  line; then the distance between projected position and green circle (the centroid) was calculated. The standard deviations are from the blue perpendicular line rather than the absolute distance, and represent how much the position varied with respect to the line. A mean (s.d.) was then calculated for each perpendicular/parallel relationship (Supplementary Fig. 1b, c). The positioning of all individuals varied more along the line than out from the line (Supplementary Fig. 1c). If the changes in position were due only to error in logger measurement, the variation in perpendicular and parallel distance and position would be expected to be equal. Because most of the variation is present along the line, the variation can be confidently attributed predominantly to bird movement, not logger noise.

**Circular statistics and phasing analysis.** Circular statistics were applied using LabVIEW (National Instruments), following that of Fisher<sup>17,34–36</sup>.

The relative positions (in the direction of flight) and phase relationships (as a proportion of the flap cycle of each 'ahead' bird) were determined for every bird following another individual. Determining appropriate independent sample criteria when considering phases is vital<sup>36</sup>, and presents a challenge when analysing phase relationships. Consider the case of two birds flying at the same relative position and at the same frequency; they would maintain the same phase relationship indefinitely. Each flap would certainly not be considered an independent sample. As a conservative alternative, we take a mean phase for any bird–bird pairing for a given area to be an independent sample; no account is taken of the length of time or number of flaps spent in the area. Perversely, this technique actually makes use of the variability in relative position, and would be poor for absolutely rigid V formations.

Statistical tests<sup>17,34–36</sup> analysed two regions, combining left and right sides: one representing V formation flight (from 0.49 to 1.49 m both spanwise and streamwise), containing the highest density of flaps; the other for nose-to-tail, streamwise flight, covering a volume  $0.25 \text{ m}$  spanwise from midline (so  $0.5 \text{ m}$  behind) and  $4 \text{ m}$  behind. This provided  $n = 165$  and  $n = 160$  bird–bird pairs for V formation and nose-to-tail regions, respectively.

The Rayleigh test was applied to determine the presence of a single unimodal direction in phase without preconceptions of any mean direction. This found a significant departure from randomness—a significant unimodal bias—in phase (whether temporal or spatial) for the V formation region. Both Rayleigh's test (parametric) and Hodges–Ajne's test<sup>17,34–36</sup> (non-parametric) on this region indicated that both the temporal and the spatial phases (taking into account the wavelength of whichever bird was ahead) were significantly different from those that would be found from a random distribution<sup>37,38</sup>.

The median phase for a given region—and its 95% confidence intervals—allows a specified alternative to be tested against. Fig. 3a, d and Supplementary Fig. 3a, b show the median statistics in graphical form for the two regions. Zero or 'in' spatial phase falls outside the 95% confidence intervals for the nose-to-tail region.

The median spatial phases for the two regions described above were used to predict the temporal phases for  $0.25\text{ m} \times 0.25\text{ m}$  along two streamwise transects using the wavelength measured for each volume along the transect. If the median spatial phase was  $\pi$ —out of phase, as it is close to in the nose-to-tail transect—we would predict it to be  $\pi$  every integer number of wavelengths, and 0 or 'in' temporal phase at  $1/2$ ,  $3/2$ ,  $5/2$ , etc. wavelengths. The model—with bounding confidence intervals due the spatial median—is shown as lines in Fig. 3a, d. Measured median temporal phases ( $\pm 95\%$  confidence intervals of the median) broadly match the predicted values (see also Supplementary Fig. 3a, b, which gives the same data in Cartesian form). Although the fit between model and observed temporal phases is visually convincing, formal statistical treatment is avoided because of uncertainty over independence between neighbouring spatial regions along the transects.

**Modelled induced flow behind flapping birds.** The implications of flap phasing in terms of potential interaction with induced flows are shown in Fig. 3c, f. For this model, it is assumed that the wingtip vortex left behind a bird ahead (the grey bird) of a follower (the black bird) follows the wingtip path through space—the convection of the vortex core (which, on average, will be inwards and downwards) is neglected<sup>39,40</sup>. Induced flow-fields are modelled following the Biot-Savart law<sup>41,42</sup>, treating the wingtip vortices as infinitely long, parallel filaments; no account is taken of variation in lift throughout the wingstroke cycle. Induced flows near the vortex cores are not modelled; these regions are represented by grey circles. They, although being correct given the reductions and assumptions described, should not be taken

as accurate quantitative calculations of the local flowfield. However, the principles they demonstrate—the strongest region of upwash and downwash close to outboard and inboard, respectively, of the wingtip path—meet basic aerodynamic expectations and recent modelling results<sup>41,42</sup>. For scale, the downwash directly between the vortices would be  $(-0.3\text{ m s}^{-1})$  between trailing vortices for behind a bird of mass 1.3 kg, span 1.2 m at a speed of  $15\text{ m s}^{-1}$  (without modelling flapping or wake contraction).

27. Barron, D. G., Brawn, J. D. & Weatherhead, P. J. Meta-analysis of transmitter effects on avian behaviour and ecology. *Methods Ecol. Evol.* **1**, 180–187 (2010).
28. Norberg, U. M. *Vertebrate Flight: Mechanics, Physiology, Morphology, Ecology and Evolution* Ch. 9, 118–132 (Springer, 2011).
29. Kaplan, E. & Hegarty, C. *Understanding GPS: Principles and Applications* Ch. 7, 304–334 (Artech House, 2005).
30. Andersson, M. & Wallander, J. Kin selection and reciprocity in flight formation? *Behav. Ecol.* **15**, 158–162 (2003).
31. Petit, D. R. & Bildstein, K. L. Development of formation flying in juvenile white ibises (*Eudocimus albus*). *Auk* **103**, 244–246 (1986).
32. Rands, S. A., Cowlshaw, G., Pettifor, R. A., Rowcliffe, J. M. & Johnstone, R. A. Spontaneous emergence of leaders and followers in foraging pairs. *Nature* **423**, 432–434 (2003).
33. Biro, D., Sumpter, D. J. T., Meade, J. & Guilford, T. From compromise to leadership in pigeon homing. *Curr. Biol.* **16**, 2123–2128 (2006).
34. Mardia, K. & Jupp, P. *Directional Statistics* Ch. 6, 94–110 (Wiley, 1999).
35. Sprent, P. & Smeeton, N. C. *Applied Nonparametric Statistical Methods* Ch. 4, 83–122 (Taylor & Francis, 2007).
36. Batschelet, E. *Circular Statistics in Biology* Chs 9, 15 (Academic, 1981).
37. Wiltschko, W. *et al.* Lateralisation of magnetic compass orientation in a migratory bird. *Nature* **419**, 467–470 (2002).
38. Holland, R. A. *et al.* Testing the role of sensory systems in the migrating heading of a songbird. *J. Exp. Biol.* **212**, 4065–4071 (2009).
39. Hubel, T. Y. *et al.* Wake structure and wing kinematics: the flight of the lesser dog-faced fruit bat, *Cynopterus brachyotis*. *J. Exp. Biol.* **213**, 3427–3440 (2010).
40. Hubel, T. Y. *et al.* Changes in kinematics and aerodynamics over a range of speeds in *Tadarida brasiliensis*, the Brazilian free-tailed bat. *J. R. Soc. Interface* **9**, 1120–1130 (2012).
41. Kroner, E. Dislocations and the Biot-Savart law. *Proc. Phys. Soc. A* **68**, 53–55 (1955).
42. Griffiths, D. J. *Introduction to Electrodynamics* Ch. 5, 215 (Prentice Hall, 1998).